AM5640 Turbulence Modelling (Jan-May 2022)
Assignment 1

AM5640 Jan-May 2022
Anand Zambare - AM21S004
Kishore Ram Sathia - ME18B085

March 16, 2022

Problem Statement

Numerically solve fully-developed turbulent channel flow using Prandtl's 1-equation model with $Re_* = u_*\delta/\nu = 395$, where $u_* = \sqrt{\tau_\omega/\rho}$ is the wall friction velocity. (Set $\rho = u_* = 1$). Use the finite difference method.

Governing Equations

Assuming the fluid is incompressible, the mean continuity equation is given by:

$$\frac{\partial \bar{u}}{\partial x} + \frac{\partial \bar{v}}{\partial y} + \frac{\partial \bar{w}}{\partial z} = 0$$

and the three RANS equations are (using Einstein's notation):

$$\frac{\partial \bar{u}_i}{\partial t} + \bar{u}_j \frac{\partial \bar{u}_i}{\partial x_j} = -\frac{1}{\rho}\frac{\partial \bar{P}}{\partial x_i} + \frac{\partial}{\partial x_j}\left\{\nu \frac{\partial \bar{u}_i}{\partial x_j}\right\} - \frac{\partial}{\partial x_j}\left\{\overline{u_i' u_j'}\right\}$$

If we assume a k-based Eddy Viscosity Model (EVM), we can write (using the Boussinesq hypothesis):

$$\overline{u_i' u_j'} = \nu_t \left(\frac{\partial \bar{u}_i}{\partial x_j} + \frac{\partial \bar{u}_j}{\partial x_i}\right) - \frac{2}{3} k \delta_{ij}$$

where $k = \frac{1}{2}\overline{u_i' u_i'}$ is the Turbulence Kinetic Energy and is obtained using the modelled Turbulence Kinetic Energy equation:

We assume that the flow is stationary ($\frac{\partial}{\partial t}$ terms vanish) and spanwise homogeneous ($\frac{\partial}{\partial z}$ terms vanish). Also, for a plane flow, $\bar{w} = 0$.
Hence the continuity and RANS equations can be simplified to:

$$\frac{\partial \bar{u}}{\partial x} + \frac{\partial \bar{v}}{\partial y} = 0 \tag{1}$$

$$\bar{u}\frac{\partial \bar{u}}{\partial x} + \bar{v}\frac{\partial \bar{u}}{\partial y} = -\frac{1}{\rho}\frac{\partial \bar{P}}{\partial x} + \frac{\partial}{\partial x_j}\left\{(\nu + \nu_t)\left(\frac{\partial \bar{u}}{\partial x_j} + \frac{\partial \bar{u}_j}{\partial x}\right)\right\} - \frac{\partial}{\partial x}\left(\frac{2}{3}k\right) \tag{2}$$

$$\bar{u}\frac{\partial \bar{v}}{\partial x} + \bar{v}\frac{\partial \bar{v}}{\partial y} = -\frac{1}{\rho}\frac{\partial \bar{P}}{\partial y} + \frac{\partial}{\partial x_j}\left\{(\nu + \nu_t)\left(\frac{\partial \bar{v}}{\partial x_j} + \frac{\partial \bar{u}_j}{\partial y}\right)\right\} - \frac{\partial}{\partial y}\left(\frac{2}{3}k\right) \tag{3}$$

$$\bar{u}\frac{\partial k}{\partial x} + \bar{v}\frac{\partial k}{\partial y} = \frac{\partial}{\partial x_j}\left\{\left(\nu + \frac{\nu_t}{\sigma_k}\right)\left(\frac{\partial k}{\partial x_j}\right)\right\} + P_k - \epsilon \tag{4}$$

The flow is fully developed, from which we get:

$$\frac{\partial \bar{u}}{\partial x} = \frac{\partial \bar{v}}{\partial x} = \frac{\partial k}{\partial x} = 0$$

Substituting in the continuity equation (1), $\frac{\partial \bar{v}}{\partial y} = 0$. Hence $\bar{v}$ is not a function of x, y or z, and so must be a constant. Since $\bar{v} = 0$ on the wall, we obtain $\bar{v} = 0$.

Equation (3) thus reduces to:

$$0 = -\frac{1}{\rho}\frac{\partial \bar{P}}{\partial y} - \frac{\partial}{\partial y}\left(\frac{2}{3}k\right)$$

Integrating throughout with respect to y:

$$0 = -\frac{1}{\rho}\bar{P} - \left(\frac{2}{3}k\right) + c_1(x)$$

Differentiating with respect to x,

$$0 = -\frac{1}{\rho}\frac{\partial \bar{P}}{\partial x} + \frac{\partial c_1}{\partial x}$$

since $\partial k/\partial x = 0$. Hence $\partial P/\partial x$ is only a function of x, not y.
Equation (2) also reduces:

$$0 = -\frac{1}{\rho}\frac{\partial \bar{P}}{\partial x} + \frac{\partial}{\partial y}\left\{(\nu + \nu_t)\left(\frac{\partial \bar{u}}{\partial y}\right)\right\} \tag{5}$$

Integrating with respect to y and rearranging:

$$-\frac{\partial \bar{P}}{\partial x}y = -\left\{(\mu + \mu_t)\left(\frac{\partial \bar{u}}{\partial y}\right)\right\} + c_2(x)$$

At $y = 0$ and $y = 2\delta$, we have $\nu_t = 0$ (see Boundary Conditions in next section), $\tau_\omega = \mu \frac{\partial \bar{u}}{\partial y}|_{y=0}$ and $-\tau_\omega = \mu \frac{\partial \bar{u}}{\partial y}|_{y=2\delta}$ by symmetry.
From these, we obtain that $c_2(x) = \tau_\omega(x)$ and:

$$\boxed{-\frac{\partial P}{\partial x} = \tau_\omega} \tag{6}$$

Setting $\rho = u_* = 1$ as per the problem statement, we get $\tau_\omega = 1$ and hence $-\frac{\partial P}{\partial x} = 1$.
Equation 4 reduces to:

$$0 = \frac{\partial}{\partial y}\left[\left(\nu + \frac{\nu_t}{\sigma_k}\right)\frac{\partial k}{\partial y}\right] + P_k - \epsilon \tag{7}$$

Equations 4 and 6 are the coupled partial differential equations for $\bar{u}$ and k. P_k and ϵ are still unknowns, which will be obtained in the subsequent section using "Prandtl's One Equation Model". Finally, these coupled equations will be solved using the Finite Difference method.

Prandtl's One Equation Model and Discretization of equations

Here the Prandtl's one equation model is used to solve for the eddy viscosity. In this model only one transport equation for the turbulent kinetic energy is solved. The rate of dissipation of turbulent kinetic energy is explicitly defined in terms of the kinetic energy, The following equations are specific to this model and the corresponding model constants (from here on, the axial mean velocity $\bar{u}$ is denoted U):

$$P_k = \nu_t(\frac{\partial U}{\partial y})^2 \qquad \nu_t = C_\mu \frac{k^2}{\epsilon} \tag{8}$$

$$C_\mu = 0.09 \qquad \sigma_k = 1.0 \qquad l_t \text{ (user defined)}$$

$$\epsilon = C_\mu \frac{k^{\frac{3}{2}}}{l_t}$$

We choose the value of l_t to be 1.0.

Using equation 7 and all the other model constants defined, the final form of the governing equations is:

$$\nu_t = k^{\frac{1}{2}} \tag{9}$$

$$\frac{\partial}{\partial y}(\nu + \nu_t)\frac{\partial U}{\partial y} = -1 \tag{10}$$

$$\frac{\partial}{\partial y}(\nu + \nu_t)\frac{\partial k}{\partial y} + \nu_t(\frac{\partial U}{\partial y})^2 - C_\mu k^{\frac{3}{2}} = 0 \tag{11}$$

Equation 8, 9 and 10 are the three important equations. The eddy viscosity ν_t is calculated from eq 8. 9 and 10 are coupled differential equations for k and U.
The finite difference scheme is used for solving the differential equations. Here the general form of the finite difference equations is used as the spacing between the nodes is not constant through out. The second derivatives are approximated using the central difference scheme and the first derivatives are also approximated using central scheme. The final form of discretized equations for U and k are as follows:

$$U_i^{n+1} = \frac{h_i h_{i+1}}{2(\nu + \nu_t^n)} + \frac{U_{i+1}^n h_{i-1} + U_{i-1}^n h_i}{h_i + h_{i+1}} \tag{12}$$

$$k_i^{n+1} = \frac{2(\nu + \nu_t^n)}{\alpha(h_i + h_{i+1})}[\frac{k_{i+1}^n}{h_i} + \frac{k_{i-1}^n}{h_{i-1}}] + \frac{\nu_t^n}{\alpha} P k_i^n \tag{13}$$

$$\text{where } \alpha = \frac{2(\nu + \nu_t^n)}{h_i h_{i+1}} + C_\mu k_i^{\frac{1}{2}}$$

Equation 11 and 12 are valid for all interior points. The equations from the boundary conditions are straightforward (as seen from the subsection Boundary Conditions).

Wilcox's $k - \omega$ model and Discretization of equations

The $k - \omega$ model considers an inverse time-scale $\omega = \epsilon/(\beta^* k)$. Hence, equation (7) becomes:

$$0 = \frac{\partial}{\partial y}[(\nu + \frac{\nu_t}{\sigma_k})\frac{\partial k}{\partial y}] + P_k - \beta^* \omega k$$

ω is calculated using:

$$0 = \frac{\partial}{\partial y}[(\nu + \frac{\nu_t}{\sigma_\omega})\frac{\partial w}{\partial y}] + \frac{\omega}{k} C_1 P_k - C_2 \omega^2$$

Dissipation rate is calculated similar to the 1-equation model as $P_k = \nu_t \left(\frac{\partial U}{\partial y}\right)^2$ and $\nu_t = k/\omega$

The value of the constants are:
$\beta^* = 9/100 \quad \sigma_k = 2 \quad \sigma_\omega = 2 \quad C_1 = 5/9 \quad C_2 = 3/40$

The final form of the discretized equations is:

$$U_i^{n+1} = \frac{h_i h_{i+1}}{2(\nu + \nu_t^n)} + \frac{U_{i+1}^n h_{i-1} + U_{i-1}^n h_i}{h_i + h_{i+1}} \tag{14}$$

$$k_i^{n+1} = \frac{[\alpha_i((h_{i-1}k_{i+1}^n) + (h_i k_{i-1}^n)) + P k_i^n]}{(\alpha_i \cdot (h_i + h_{i-1})) + (0.09\omega_i^n)} \tag{15}$$

$$\omega_i^{n+1} = \frac{[\alpha_i((h_{i-1}\omega_{i+1}^n) + (h_i \omega_{i-1}^n)) + P k_i^n]}{(\alpha_i \cdot (h_i + h_{i-1})) + (\frac{3\omega_i^n}{40}) - \frac{5Pk_i^n}{9K_i^n}} \tag{16}$$

Boundary Conditions

The no-slip boundary condition at the wall implies that both the mean and fluctuating components of velocity at the wall are identically zero. Hence:

$$U_{\omega=0} = U_{\omega=2\delta} = 0$$

$$k_{\omega=0} = k_{\omega=2\delta} = 0$$

since $k = \frac{1}{2}\overline{u_i' u_i'}$

In the One-Equation Model, since $\nu_t = C_\mu \frac{k^2}{\epsilon}$ and $\epsilon = C_\mu \frac{k^{\frac{3}{2}}}{l_t}$, we obtain that the eddy viscosity ν_t is also 0 at the walls. This was used earlier when deriving the condition that $\partial P/\partial x = \tau_\omega$ at the wall.

In the $k - \omega$ model also, as $y \to 0$, $k/\omega \to 0$. Hence the derivation for the condition $\partial P/\partial x = \tau_\omega$ at the wall is still valid. The boundary condition implementation for ω is tricky. This model uses an explicit equation for the near wall values of the ω . The following boundary condition is used for ω : For $Y^+ \leq 3$

$$\omega = \frac{6\nu}{y^2 C_2} \text{ where, } C_2 = \frac{3}{40}$$

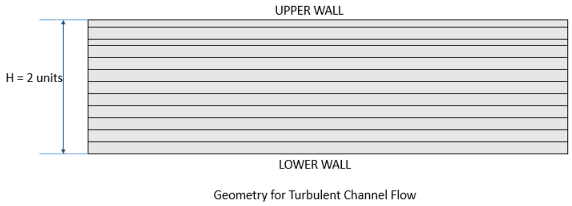

Figure 1: Geometry for Turbulent Channel Flow

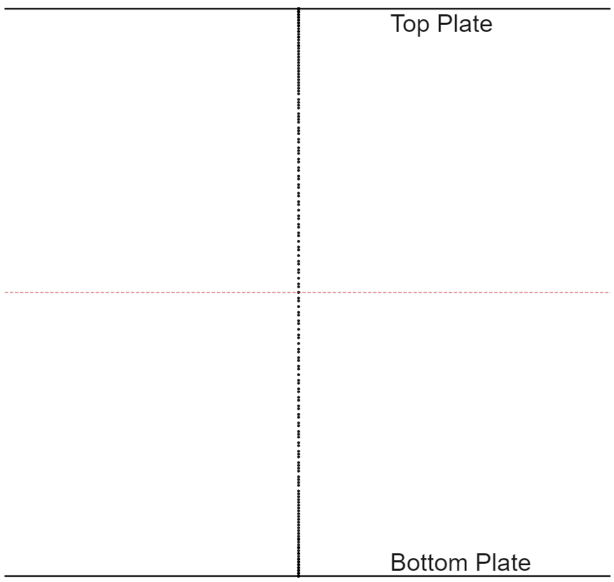

Figure 2: Distribution of nodes for finite difference calculation

The nodes are non-evenly spaced, denser close to the walls and sparse close to the mid-line.

Error and Tolerance

Initial conditions are always very tricky and important for turbulence models: the simulation will not start if we initialize all the variables to 0. The initial conditions and inflow conditions have impact on the number of iterations required for convergence too.

The laminar solution for U to the problem is a parabola with maximum velocity. Thus the initial velocity at the various nodes was chosen to be (for simplicity) varying linearly from the plates to the mid-line. The value of the velocity at the mid-line is initially unknown, and by trial-and-error, the value 0.5 seemed to minimize the number of iterations.

The initial value for the turbulence kinetic energy k was guessed to be of the order of 1% of the initial mid-line velocity, hence initially $k = 0.005$.

The Gauss Seidel method is used to solve the system of equations. The solution is said to have converged once the residual of k (defined as follows) falls below a tolerance of 10^{-4}.

$$\text{residual} = \sum_{i=1}^{n} |k_{current}[i] - k_{prev}[i]|$$

Results

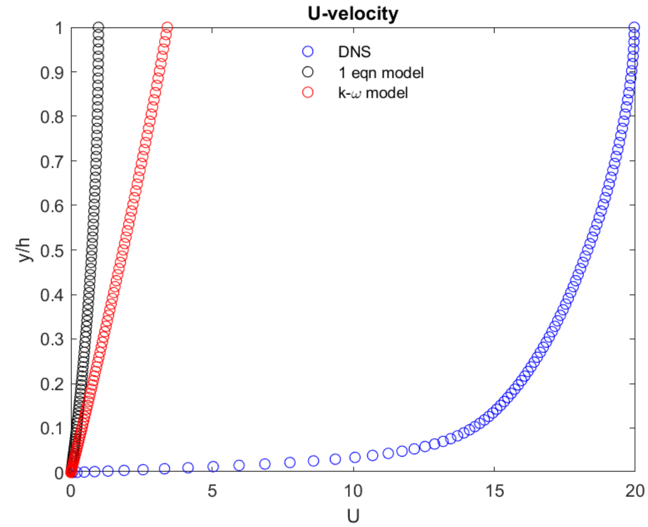

Figure 3: U-velocity

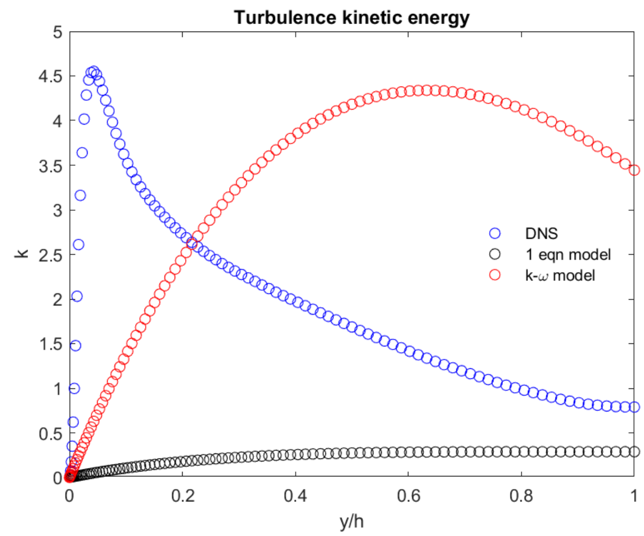

Figure 4: Turbulence Kinetic Energy

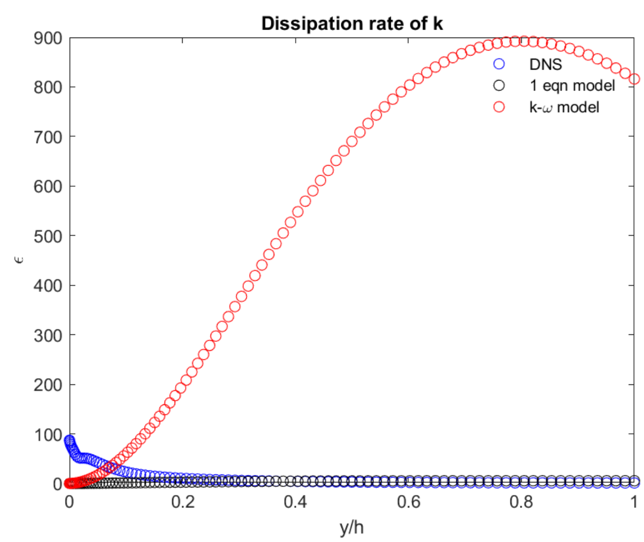

Figure 5: Dissipation rate ϵ

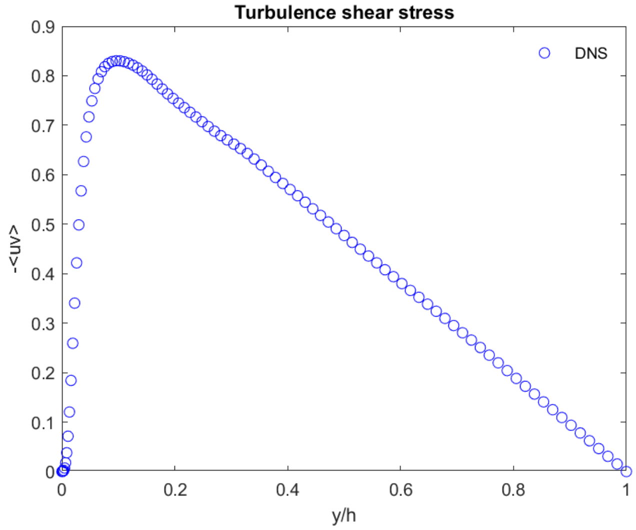

Figure 6: Turbulence shear stress

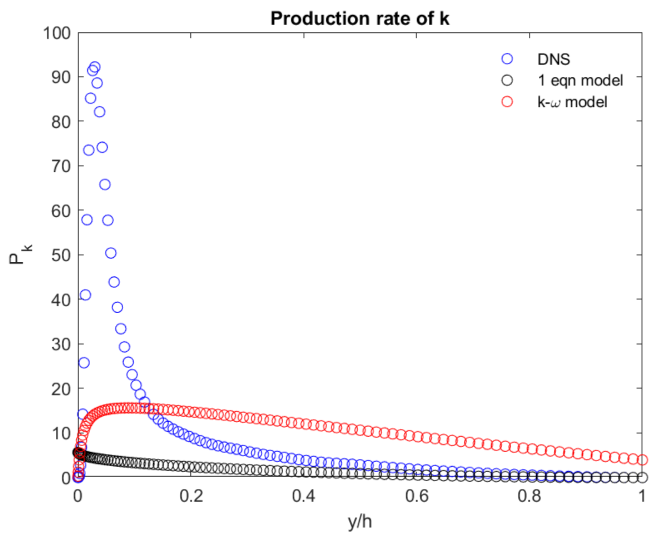

Figure 7: Production Rate P_k

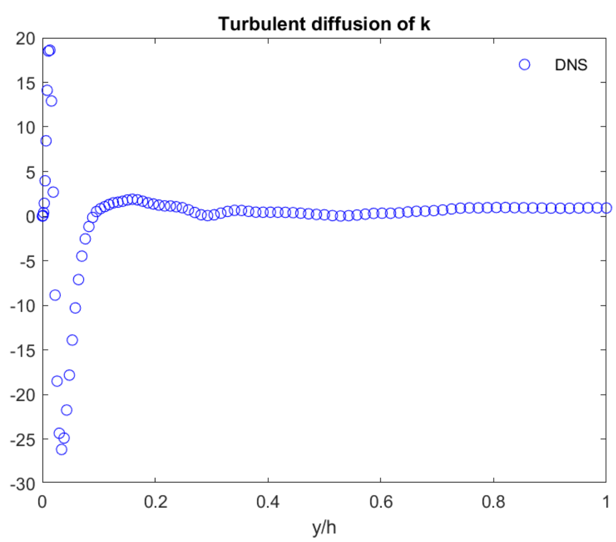

Figure 8: Turbulent diffusion of k

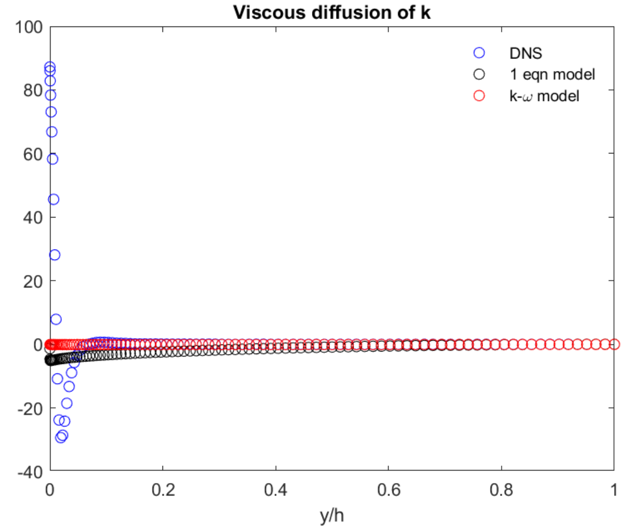

Figure 9: Viscous diffusion of k

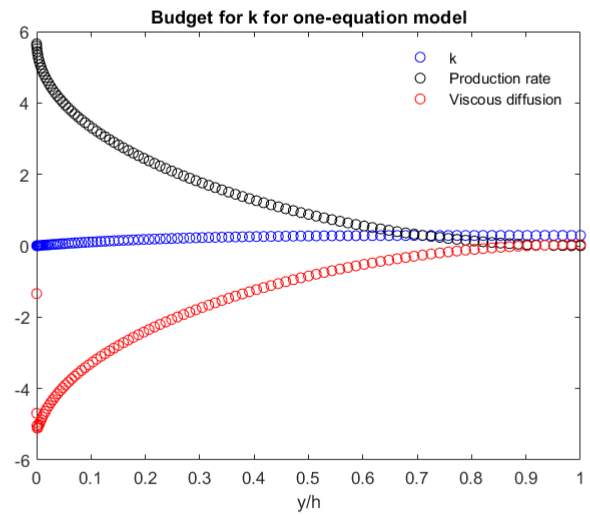

Figure 10: Budget of k for one-equation model

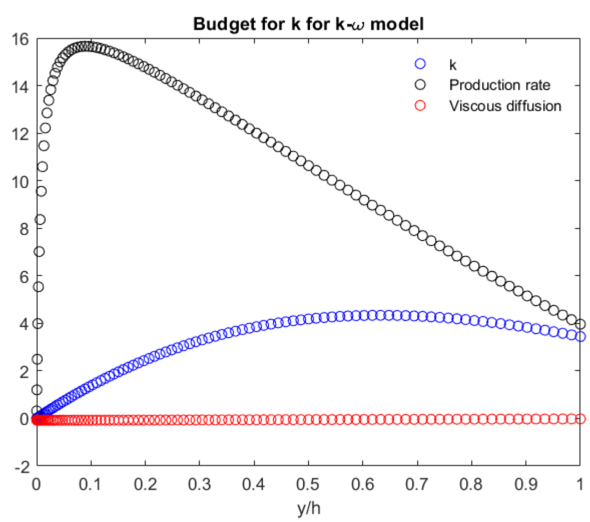

Figure 11: Budget of k for $k-\omega$ model

Plotting turbulent shear stress and the turbulent diffusion of turbulence kinetic energy k require knowledge of the fluctuating components of velocity u', v', w', which are not being calculated in either the One-equation model or the $k - \omega$ model. Hence, only the DNS data is plotted for these two plots.

Observations and Conclusion

We observe from the plot of U that the velocity at the mid-line predicted by various models is different from the value obtained using the DNS data, even though the velocity curves show a similar shape in all 3 cases: the two models and DNS.

From the budget of the turbulence kinetic energy, it is clear that the behaviour of the model and DNS matches away from the wall. Near the wall more grid points might be required (increasing required computational efforts) or a better modelling approach is required (say, using wall functions). Since the models do not behave appropriately near the wall, phenomena such as drag, lift etc. which is concerned with wall behaviour should not be analyzed through such modeling techniques. Different models can be used with better behaviour near wall for drag-lift calculations.